Effects of Organic Material on Magnetoresistance in Electron-doped Double Perovskite

Ya Fang Li (missli1129@163.com)
Henan Normal University https://orcid.org/0000-0002-3325-9129
Yu Liu
Henan Normal University
Yan-Ming Zhang
Henan Normal University
Jin-Feng Wang
Henan Normal University

Research Article

Keywords: La0.5Sr1.5FeMoO6 double perovskite, Inorganic/organic composite, Magnetoresistance, Grain boundary

Posted Date: March 18th, 2021

DOI: https://doi.org/10.21203/rs.3.rs-297068/v1

Effects of organic material on magnetoresistance in electron-doped double perovskite

Ya-Fang Li*, Yu Liu, Yan-Ming Zhang and Jin-Feng Wang*

*Corresponding author

College of Physics, National Demonstration Center for Experimental Physics Education, Henan Normal University and Henan Key Laboratory of Photovoltaic Materials, Xinxiang 453007, China

Email: missli1129@163.com (Ya-Fang Li） or jfwang@htu.edu.cn (Jin-Feng Wang)

Abstract. The Curie temperature of electron-doped Sr_2FeMoO_6 can be optimized significantly due to the band-filling effect, but accompanying an almost absent low-field magnetoresistance (LFMR), which is unfavorable to applications in the magnetoresistive devices operated at room-temperature. Our previous works confirmed that, a remarkable enhanced LFMR was observed in Sr_2FeMoO_6 by modifying the grain boundary with insulating organic small molecules (glycerin, $CH_2OHCHOHCH_2OH$). However, in this work, modifying the grain boundary strength of the $La_{0.5}Sr_{1.5}FeMoO_6$ with the insulating organic macromolecules (oleic acid, $CH_3(CH_2)_7CH=CH(CH_2)_7COOH$) or small molecules (glycerin), both of them have negligible functions on the magnetoresistance behavior in $La_{0.5}Sr_{1.5}FeMoO_6$. Contrary to the glycerin-modified Sr_2FeMoO_6, Sr_2FeMoO_6/oleic acid composites don't exhibit an obviously increased magnetoresistance property. Based on the above experimental results and the related works, it is proposed that, maintaining high spin polarization of the carriers at the Fermi level and improving the tunneling process across the grain boundary by using the suitable organic materials are decisive factors for optimizing the magnetoresistance behavior in the similar electron-doped double perovskites.

Key words: $La_{0.5}Sr_{1.5}FeMoO_6$ double perovskite; Inorganic/organic composite; Magnetoresistance; Grain boundary

Declarations

Funding This work was supported by fund from the Natural Science Foundation of China (U1504107).

Conflict of interest The authors declare that there is no conflict of interest.

Relevance Summary

1. The Curie temperature of electron-doped Sr_2FeMoO_6 can be optimized significantly but always accompanying an almost absent of low-field magnetoresistance, which is unfavorable to applications in the magnetoresistive devices operated at room-temperature.
2. In this work, the transport and magnetic properties of $La_{0.5}Sr_{1.5}FeMoO_6$ modified by organic materials are discussed systematically. And we may provide an effective method to solve the problem.

1 Introduction

Due to its a half-metallic property with the 100% spin-polarization at the Fermi level, a high Curie temperature (T_C) of ~415 K and remarkable large low-filed magnetoresistance (LFMR) behavior, double perovskite Sr_2FeMoO_6 (SFMO) has been paid a great deal of attention in views of its critical fundamental investigation values and immense potential technological applications for spintronic and magnetoresistive devices operated at room temperature [1].

It is well known that in an ideal SFMO double perovskite structure, the FeO_6 and MoO_6 octahedral arrange alternatively along the three axes of tetragonal structure with the Sr cations occupy the voids between them. Strong antiferromagnetic correlation exists between the localized magnetic moments (Fe^{3+}: $3d^5$) and the delocalized electron (Mo^{5+}: $4d^1$) in a double-exchange-like type, the magnetic coupling induces a ferrimagnetic state with an ideal saturated magnetization (M_S) of 4 $\boldsymbol{\mu_B}$ per formula unit [2-7]. The strength of magnetic coupling in SFMO double perovskite is mainly controlled by the carrier density at the Fermi level, so it indicates that doping electrons in the conduction band is an effective way to enhance T_C [8-14]. This point was confirmed by a substantial enhancement of T_C more than 80 K in $La_xSr_{(2-x)}FeMoO_6$ [9]and $(Ba_{0.8}Sr_{0.2})_{2-x}La_xFeMoO_6$ materials [15]. Obviously, the celebrated strategy increases the operating temperature range of the electromagnetic applications in SFMO double perovskite. However, the increased T_C in electron-doped double perovskites always accompany with a strong suppression on MR effect [9, 15, 16]. This phenomenon seriously affects functional properties of materials and constrains the technical application. Hence, it is necessary and meaningful to improve the MR effect in electron-doping SFMO system.

As a fact, a remarkable large MR effect can be observed in polycrystalline SFMO ceramics, but it is almost absent in SFMO single crystals or epitaxial films [17-19]. This suggests that the LFMR of

SFMO is a type of tunneling magnetoresistance, the transport process is related with the spin-dependent scattering occurred at magnetic domain boundaries, so the existence of grain boundary in SFMO is vital for magnetoresistance [1]. Previous research proved that LFMR could be improved by enhancing the GB strength in many methods, such as adding the second phase in GB [20, 21], slightly oxidizing GB [22, 23], reducing the grain size [24, 25] and dispersing the grain uniformly [26]etc. It should be noted that there are three common points in these methods. First, the increment of LFMR value always accompanies with the enhancement of resistivity. Actually, a function of $\boldsymbol{\rho \propto exp(\gamma s\sqrt{\Delta})}$ was proposed to express the strength of the GB insulating barriers. From this, the GB strength is directly measured by $\boldsymbol{\rho}$ [27]. Second, the increment of LFMR value always with the decrement of magnetization. Moreover, the experiment process of above methods is relatively complex. Therefore, it is necessary to establish a facile method which can maintain the magnetization while improve the LFMR value of SFMO. In our previous research, the SFMO ceramic was soaked in organic matter, by the method directly, the resistivity was increased about 500 times and the LFMR value was effectively improved up to -29.5% at 10 K [28]. Based on the achievement, we infer that the method of preparing $La_{0.5}Sr_{1.5}FeMoO_6$ (LSFMO)/organic matter composites could be used to eliminate the negative effect resulting from electrons doping in SFMO ceramics and then optimize the LFMR effect while ensuring the magnetization.

The organic matters of oleic acid ($CH_3(CH_2)_7CH=CH(CH_2)_7COOH$) and glycerin ($CH_2OHCHOHCH_2OH$) were used as the modifying material in this work. The oleic acid has a long-chain structure with the molecular weight of 282.45 and the glycerin has a short-chain structure with the molecular weight of 92.09. It is obvious that the former has the more excellent insulation.

In this work, three composites of LSFMO/oleic acid, LSFMO/glycerin and SFMO/oleic acid were prepared to investigate the effect of organic materials on the magnetoresistance behavior in electron-

doped double perovskite. The structure, magnetization, electrical resistivity and magnetoresistance of composites were investigated systematically and comparatively. The main results indicate that neither of the MR behavior in the three experiments has been optimized effectively. It proves that it is critical to select a suitable organic material to modify GB while maintain the high spin polarization of the carriers at the Fermi level in the electron-doped double perovskite.

2 Experimental

2.1 The method of Experiment I ($La_{0.5}Sr_{1.5}FeMoO_6$/oleic acid composite)

$La_{0.5}Sr_{1.5}FeMoO_6$ ceramics were synthesized by a conventional solid-state reaction method. First, the appropriate amounts of analytic grade La_2O_3, $SrCO_3$, Fe_2O_3 and MoO_3 powders were weighted, ground 3 h in an agate mortar and sintered at 900 ℃ for 10 h in air. The sintered powder was ground again and then pressed into disks. After that, these disks were annealed at 1200 ℃ for 12 h in the 5% H_2/95% Ar reducing atmosphere. Pure LSFMO powder was collected after triturating these annealed disks.

To modify the GB strength, the as-prepared pure LSFMO powder was post-treated as follows: first, different volume proportions of the oleic acid ($CH_3(CH_2)_7CH=CH(CH_2)_7COOH$, V_1) and alcohol (V_2) were fully stirred to form the mixed solution (V=0, 0.1, 0.2, 0.3, 0.4, 0.5,$\boldsymbol{V = V_1/V_1 + V_2}$). For each treatment, 20 $\boldsymbol{\mu L}$ of the mixed solution was pipetted and added into 0.2 g as-prepared LSFMO powder. After six pipetting times, the formed organic/inorganic composite was thoroughly admixed and pressed into disk, then conserved at room temperature (RT). The collected composites were labeled as C1-C6, respectively.

2.2 The method of Experiment II ($La_{0.5}Sr_{1.5}FeMoO_6$/glycerin composite)

For contrasting with Experiment I, in this experiment, the modificatory factor oleic acid was

substituted by glycerin ($CH_2OHCHOHCH_2OH$). Pure LSFMO powder (in Experiment I) was pressed into disks and the mass of every disk was 0.2 g. To control the participating content of glycerin at GB, the disks were soaked in the isometric mixed reagent of glycerin and alcohol under the protection of N_2, and kept static at room temperature for 5 and 15 days. Subsequently, the disks were taken out and gently washed three times by alcohol, dried in vacuum condition at RT. The collected disks were labeled as C7 (5 days) and C8 (15 days).

2.3 The method of Experiment III (Sr_2FeMoO_6/oleic acid composite)

The modified object LSFMO was substituted by pure SFMO. Specifically, the suitable amounts of analytic grade $SrCO_3$, Fe_2O_3 and MoO_3 powders were weighted, ground and sintered at 900 ℃ for 10 h in air. Then the sintered powder was ground again for 3 h and annealed at 1200 ℃ for 12 h in 5% H_2/95% Ar reducing atmosphere. To modify the GBs, 0.2 g of SFMO powder was mixed homogeneously with 20 $\boldsymbol{\mu L}$ isopyknic mixed reagent of oleic acid and alcohol solution here. After completely admixing, the composite was pressed into disk and conserved at RT. The collected disk was labeled as C9.

Room-temperature X-ray diffraction (XRD) experiments were performed by using Bruker D8 Discover. The microstructure of the samples was examined through high resolution field emission scanning electron microscope (FESEM). The C element's distribution was carried out using energy dispersive X-ray spectroscopy (EDS) coupled with FESEM instrument. The magnetization and magnetic transport data of all samples (C1-C9) were carried out by a physical property measurements system (PPMS Quantum Design).

3 Results and discussion

The crystal structure of all prepared polycrystalline samples was detected by the X-ray diffraction (Fig. 1). From the picture, it can be clearly seen that all the ceramics were well consistent with tetragonal space group of I4/m. Neither XRD peak shifting nor other impurities can be observed in the composites. It manifests that the organic molecules are mainly located at grain boundaries and have any effect on the structure of original samples. Otherwise, it can also be interpreted as there was negligible or even no chemical reaction between them. $SrMoO_4$ as a common second phase exists in SFMO double perovskite can be obtained by oxidation [23, 29] or sonication process [30] in experiments. However, such a secondary phase is not shown up in this work which is evidenced by XRD results. The discrepancies between the present study and the previous one [29] may result from the different experimental manipulations, like the prepared method of samples and the content of the solvent in organic matter.

Fig.2 shows the FESEM images for pristine LSFMO (C1) and LSFMO/oleic acid composites (C2-C6). The FESEM images show the grain size about 2.5 **μm** in all composites. The phenomenon that LSFMO grains with small size are inlaid in measured areas can be observed in these images. This is attributed to the physical mixing process. In this process, the LSFMO's binding force forming in the annealing time is destroyed by the external pressure and then grains are dispersed, although they are subsequently pressed into disks again, it cannot distribute uniformly like the annealed samples. The C element' distributions in these samples measured with EDS are shown in the insets in Figure 2. It can be observed that the content of oleic acid increases with the increment of the *V* values. Based on the FESEM and EDS measurements, it is reasonable to conclude that the physisorption of oleic acid in LSFMO grain regions might be the dominant states, which is also confirmed by the XRD analysis.

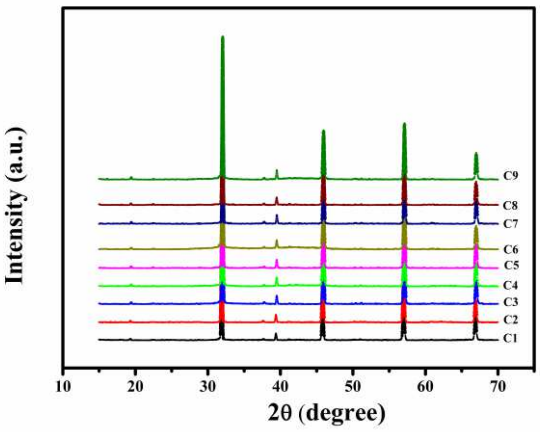

Fig. 1 The XRD patterns of all prepared ceramics (C1-C9)

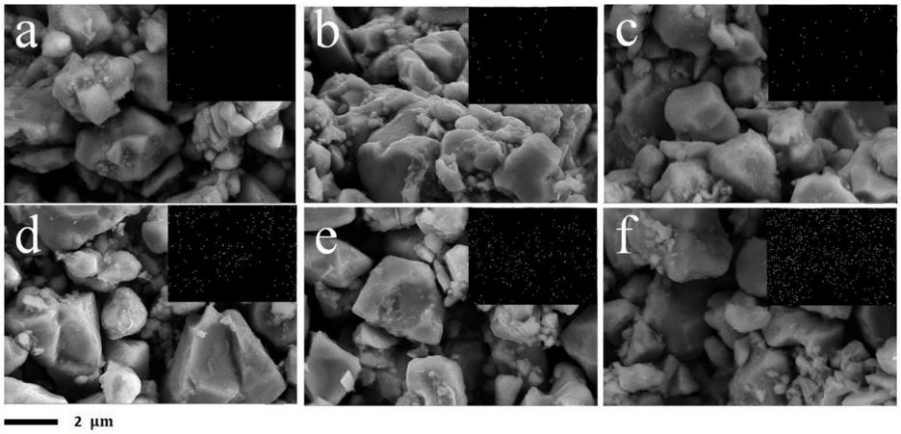

Fig. 2 FESEM images of oleic acid/$La_{0.5}Sr_{1.5}FeMoO_6$ composites, (a-f) correspond to C1-C6 samples. The insets are the corresponding C element mappings

The magnetic hysteresis loops of LSFMO with different volume proportions of oleic acid/alcohol solution (V=0, 0.1, 0.2, 0.3, 0.4, 0.5) composites were measured at 50 K and 300 K, shown in Fig. 3 and 4 respectively. Evidently, all the samples show the ferromagnetic nature with a well-saturated feature between -2.5 T and +2.5 T. The mass differences of the pure LSFMO with LSFMO/oleic acid composites are provided in Table 1. It can be observed that the mass of organic matter that entered into LSFMO grain boundaries is too little and this extra mass has negligible effect when we calculate the magnetization values. With the oleic acid content increasing, the M_S values at 50 K are respectively 1.46, 1.41, 1.68, 1.33, 1.32 and 1.47 $\boldsymbol{\mu_B/f.u.}$ of the corresponding C1-C6 composite samples, which suggests the organic

material can maintain the magnetization. Accompanying with the similar coercive field, although oleic acid molecules segregate at the grain boundaries, they have no obvious effect on the LSFMO ferromagnetic domains. An analogous behavior appears in the M-H curves at 300 K (Fig.4).

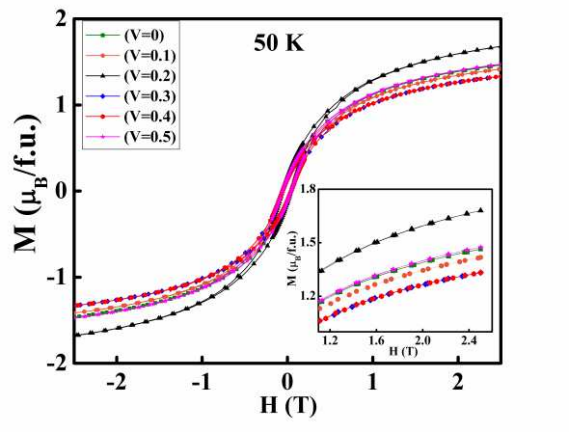

Fig. 3 The magnetization versus magnetic field (M-H) curves measured at 50 K for Experiment I. The inset is the locally enlarged M-H curves

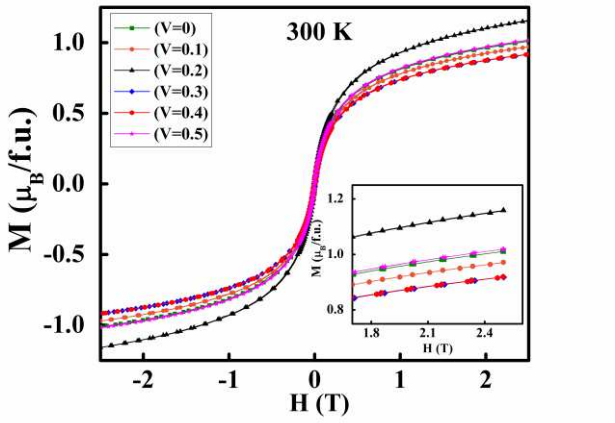

Fig. 4 The magnetization versus magnetic field (M-H) curves measured at 300 K for C1-C6 in Experiment I. The inset is the locally enlarged M-H curves

Table 1 The mass differences of the pure LSFMO with LSFMO/oleic acid composites

Sample	C1	C2	C3	C4	C5	C6
Mass before soaking (g)	0.2000	0.2000	0.2000	0.2000	0.2000	0.2000
Mass after soaking (g)	0.2000	0.2002	0.2008	0.2011	0.2027	0.2036
Mass difference (%)	0%	0.10%	0.40%	0.55%	1.35%	1.80%

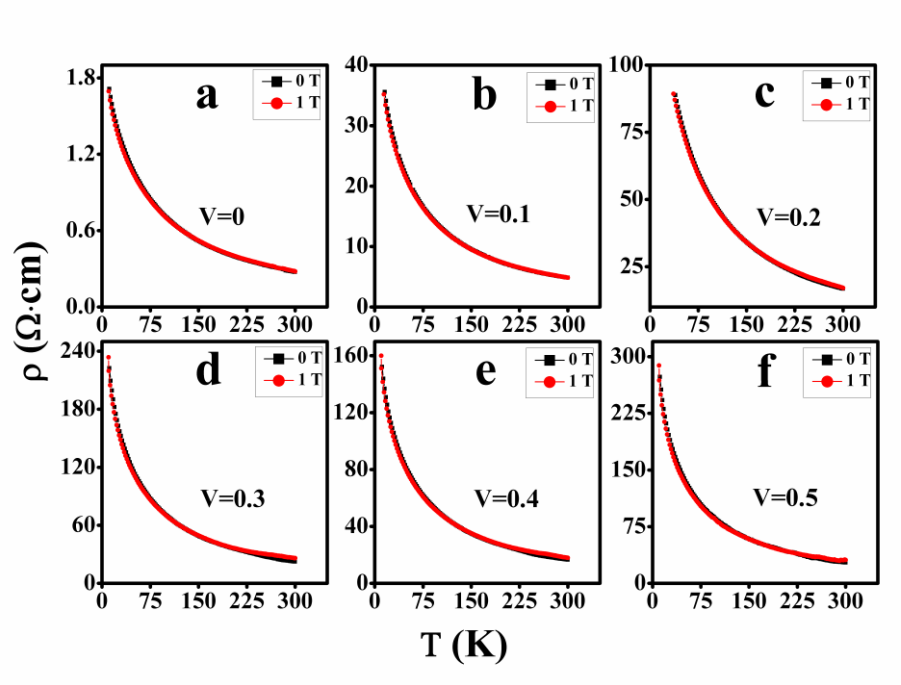

Fig. 5 Temperature dependent resistivity curves for C1-C6 (a-f) measured at 10 K-300 K with 0 T and 1 T extra field

Fig. 5 shows the temperature dependent resistivity curves for C1-C6 composites with 0 T and 1 T extra field. All the ceramics exhibit a semiconductor-like behavior in the range of investigating. In this system, it can be observed a systematic enhancement in resistivity over the whole temperature range of 10-300 K while adding the extra amount of oleic acid without reducing the SFMO content. The measured curves with 0 T and 1 T are almost overlapped in this figure, it suggests extra field has no obvious influence on resistance property. In order to describe resistivity more directly, the resistivity values (without extra field) of C1-C6 at 50 K and 300 K are shown (Fig. 6) In this picture, values of C6 composite are 138.8 Ω cm and 27.5 Ω cm at 50 K and 300 K respectively, exhibiting ~130 times and ~100 times of C1 (1.0661 Ω cm at 50 K, 0.27 Ω cm at 300 K). The variation of resistivity implies that the charge transport is significantly influenced by the nature of GB, it can be explained by that oleic acid effectively weak the tunneling conduction ability of charger carriers when they across the grain boundaries. The jump points in C5 composite (V=0.4) may result from the preparation process.

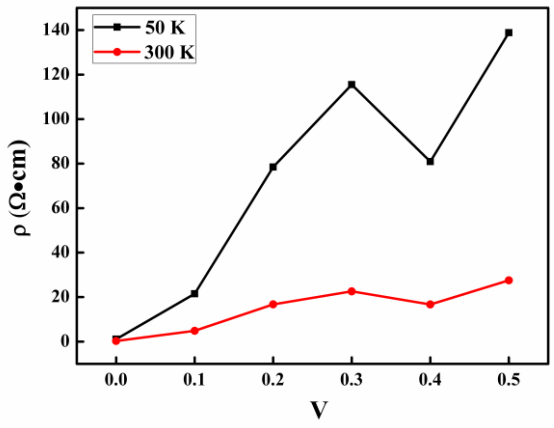

177

178 **Fig. 6** The resistivity-volume proportions curves of samples (C1-C6) at 50 K and 300 K with zero-field

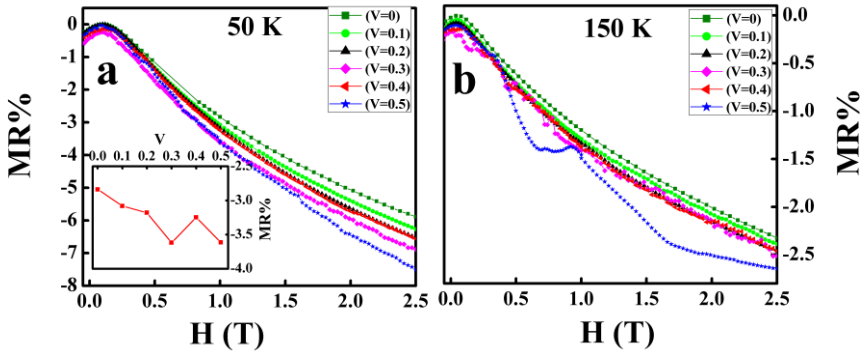

179

180 **Fig. 7** MR% versus applied magnetic field plots of $La_{0.5}Sr_{1.5}FeMoO_6$ with different volume proportions of oleic
181 acid/alcohol contents (V=0, 0.1, 0.2, 0.3, 0.4, 0.5) measured at 50 K (a) and 150 K (b). The inset in (a) was the
182 volume proportions dependent MR at 1 T

183 MR% versus applied magnetic field (MR%-H) curves for C1-C6 at 50 K and 150 K were depicted
184 in Fig. 7a and Fig. 7b, respectively. The MR% is defined here as $\boldsymbol{MR\%} = (\boldsymbol{\rho_H} - \boldsymbol{\rho_0})/\boldsymbol{\rho_0} \times \mathbf{100}\%$,
185 where $\boldsymbol{\rho_H}$ and $\boldsymbol{\rho_0}$ are the values of resistivity with and without a magnetic field. From figure 7, the MR%
186 value is slightly enhanced with the organic matter content, but the enhancement is negligible when
187 compare with other researches [28-32]. From the inset in Fig. 7a, the LFMR (H=1 T) value of C1
188 composite at 50 K is -2.8% and it gets to the maximum -3.6% of C6, it just improves 0.8%. Moreover,
189 the same phenomenon occurred at 150 K, depicted in Fig. 7b. These data can strongly prove that the
190 method of modifying LSFMO by organic matter is not available to improve LFMR response. This result
191 violates the previous inference which is the stronger GB strength portend higher MR. To make our result

compelling, more in-depth comparisons and discussions will be addressed in next content.

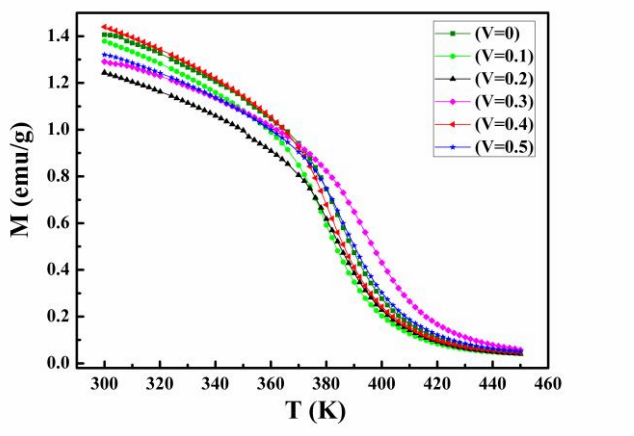

Fig. 8 Magnetization-temperature (M-T) curves for C1-C6 measured from 300 K to 450 K

Fig. 8 shows the magnetization versus temperature plots of C1-C6 composite samples that measured from 300 K to 450 K. Almost samples undergo a ferromagnetic to paramagnetic transition at the same temperature (~420 K). By adding the oleic acid molecules in GB, there is no obvious change in the magnetic transition temperature of samples. This is yet another confirmation that the organic matter is not beneficial to enhance the ferromagnetic coupling strengths of the LSFMO material.

It is expected that, the insulating big molecules (oleic acid) located at GBs of LSFMO double perovskite can increase the tunneling probability of spin electrons, and thus enhance the LFMR behavior. Unfortunately, according to the analysis with Experiment I, we conclude that the method is not workable. However, a remarkable LFMR enhancement in SFMO modified with small molecules (glycerin) was observed in our previous study, in which the LFMR of SFMO/glycerin composite was more than 2 times larger than that of the pure SFMO [28]. Therefore, we designed Experiment II (LSFMO/glycerin) to further study.

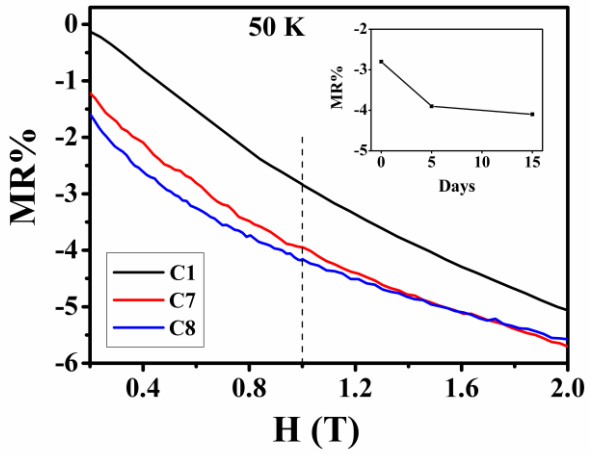

Fig. 9 MR% versus applied magnetic field of C1, C7 and C8 measured at 50 K (Experiment II). The inset is the LFMR value at 1 T of C1, C7 and C8

In order to understand the effect of glycerin molecules on LSFMO, the MR% versus applied magnetic field curves are presented in Figure 9. Since the content of glycerin in grain boundary increased with soaking time, the LFMR effect must grow consistently as well as the GB strength. However, from the inset, the LFMR at 50 K of C1, C7, C8 composites are -2.8%, -3.9% and -4.1% respectively. It is obviously that the LFMR effect of LSFMO/glycerin composite cannot also be optimized very well, which has a sharp contrast with SFMO/glycerin [28]. The difference between them may lie in that, La electrons doped at Sr sites leads to two effects: one is band-filling effect, and the other is the increased Fe/Mo anti-site defects concentration, both of them can decrease the amounts of spin-polarized electrons that tunneling across GB. So, we can conclude that maintaining high spin polarization of the carriers at the Fermi level is a crucial factor to obtain an excellent MR behavior in similar electron-doped double perovskite.

Based on the experiments, we noticed that it is necessary to maintain a high spin polarization of carriers to obtain a large MR effect. In Experiment III, we prepared the SFMO with a high Fe/Mo ordering degree to ensure a high spin polarization of carriers at the Fermi level, and then fabricate it with the oleic acid molecule.

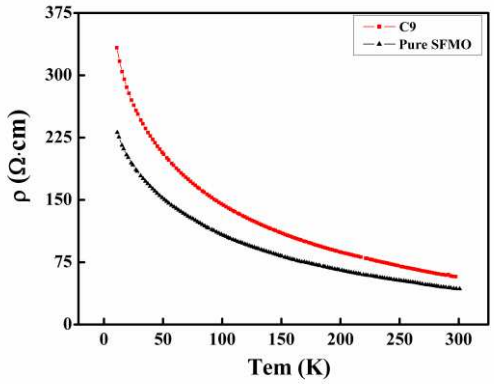

225

226 **Fig. 10** Resistivity versus temperature curves for pure SFMO and C9 at 10 K-300 K with zero-field

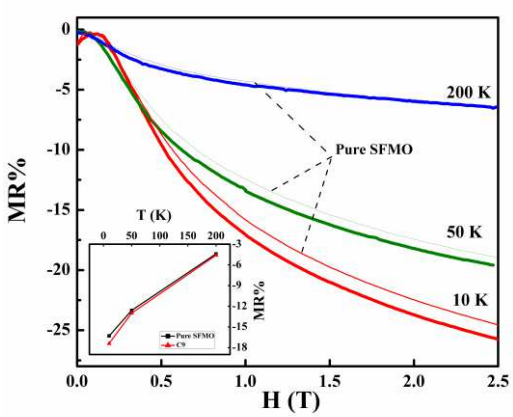

227

228 **Fig. 11** MR% versus applied magnetic field of pure SFMO sample (*thin lines*) and C9 (*thick lines*) measured at
229 10 K, 50 K and 200 K. The inset in figure is the measured temperature dependent low field magnetoresistance
230 at 1 T for the two samples

231 It can be directly gotten from Fig. 10 that the resistivity of SFMO can be enhanced by introducing
232 oleic acid in the whole temperature range, similarly with the previous statement. The MR of the pure
233 SFMO (thin lines) and C9 composite (thick lines) were measured at 10 K, 50 K and 200 K, shown in
234 Figure 11. As the picture presents, the LFMR of pure SFMO at 1 T are -16.3%, -12.6%, -4.4%
235 respectively and -17.4%，-13.0%，-4.6% for C9 in 10 K, 50 K and 200 K. It is obvious that the SFMO
236 modified by oleic acid still cannot effectively optimize the LFMR. Otherwise, this behavior is in a sharp
237 contrast with the SFMO/glycerin work [28]. Therefore, we noticed that the different results may due to
238 the different molecular structure and insulation properties of oleic acid and glycerin.

Organic molecules have been already acknowledged as the suitable spin transport medium in magnetic materials [33-36]. In these works, the chemical bonding between organic molecules and ferromagnetic grains is the decisive factor for the enhancement of LFMR. Oleic acid is recognized as an efficient barrier when it closely contacts with the Fe_3O_4 or $La_{0.7}Sr_{0.3}MnO_3$ grains with a single molecular layer. But this phenomenon has not happened in our present work. It may derive from that oleic acid molecule is physically bonded with SFMO grains.

An efficient optimization of LFMR have been observed in SFMO/glycerin [28], which has a sharp contrast with SFMO/oleic acid. The reasons maybe lie in the different molecular structure of the organic matter and bonding strength between organic molecules and SFMO grain boundary. As for SFMO/oleic acid, it is difficult to form a single layer between two grains due to big molecule oleic acid and different preparation process compared with Fe_3O_4 or $La_{0.7}Sr_{0.3}MnO_3$ grains, thus the stronger energy barrier between oleic acid big molecule and SFMO grain will weak the spin injection efficiency and therefore suppress to LFMR effect. But in the SFMO/glycerin system, compared with oleic acid, glycerin has a smaller molecular size and three hydroxyl groups, leads to a relative strong bonding strength with the SFMO interfacial grain. Therefore, glycerin is beneficial to spin injection and the improvement of LFMR effect.

Based on the analysis, we conclude that oleic acid can be recognized as a suitable transport medium when it chemically bonds to ferromagnetic grain. But when it bonds in physically, like the present work, oleic acid cannot optimize efficiently LFMR of the SFMO. In this case, it's available to select the smaller organic molecule with many hydroxyl groups to modify GB to enhance LFMR in the similar double perovskite materials.

4 Conclusion

$La_{0.5}Sr_{1.5}FeMoO_6$/oleic acid composite was prepared to expect to improve the magnetoresistance of $La_{0.5}Sr_{1.5}FeMoO_6$ electron-doped double perovskite in Experiment I, but the result shows that the modifying treatment is noneffective. In order to make it clear, $La_{0.5}Sr_{1.5}FeMoO_6$/glycerin composite (Experiment II) and Sr_2FeMoO_6 /oleic acid composite (Experiment III) were designed and the MR behavior were detailedly disscussed respectively. Contrary to the glycerin-modified Sr_2FeMoO_6 which has made a remarkable enhanced LFMR in our previous works, both of the composites in Experiment II and III don't exhibit the obviously increased MR. Based on the analysis of the experiments and the related works, we conclude the invalid MR effect on $La_{0.5}Sr_{1.5}FeMoO_6$/oleic acid composite results from two respects: the lower spin polarization of carriers at the Fermi level and the weaker spin injection efficiency in GB derived from the oleic acid macromolecule. Maybe our work provides a direction for the MR enhancement of electron-doped double perovskite: it is necessary to maintain a high spin polarization in materials and select the small organic molecule to improve the tunneling process across GB. The further work is certainly required and we believe this is an interesting topic for future work.

References

[1] K.I. Kobayashi, T. Kimura, H. Sawada, K. Terakura, Y. Tokura, Nature 395, 677 (1998)

[2] L. Balcells, J. Navarro, M. Bibes, A. Roig, B. Martínez, J. Fontcuberta, Appl. Phys. Lett. 78, 781 (2001)

[3] J. Navarro, J. Nogués, J.S. Muñoz, J. Fontcuberta, Phys. Rev. B 67, 174416 (2003)

[4] Z. Wang, A.H. Tavabi, L. Jin, J. Rusz, D. Tyutyunnikov, H. Jiang, Y. Moritomo, J. Mayer, R.E. Dunin-Borkowski, R. Yu, J. Zhu, X. Zhong, Nat. Mater. 17, 221 (2018)

[5] I. Hussain, M.S. Anwar, S.N. Khan, J.W. Kim, K.C. Chung, B.H. Koo, J. Alloys Compd. 694, 815 (2017)

[6] S. Varaprasad, K. Thyagarajan, Y. Markandeya, K. Suresh, G. Bhikshamaiah, J. Mater. Sci. : Mater. Electron. 29, 13606 (2018)

[7] L.D. Hien, N.P. Duong, L.N. Anh, T.T. Loan, S. Soontaranon, A. de Visser, J. Alloys Compd. 793, 375 (2019)

[8] M. Tovar, M.T. Causa, A. Butera, J. Navarro, B. Martínez, J. Fontcuberta, M.C.G. Passeggi, Phys.

Rev. B 66, 024409 (2002)
[9] J. Navarro, C. Frontera, L. Balcells, B. Martínez, J. Fontcuberta, Phys. Rev. B 64, 092411 (2001)
[10] J. Fontcuberta, D. Rubi, C. Frontera, J.L. García-Muñoz, M. Wojcik, E. Jedryka, S. Nadolski, M. Izquierdo, J. Avila, M.C. Asensio, J. Magn. Magn. Mater. 290-291, 974 (2005)
[11] C. Frontera, D. Rubi, J. Navarro, J.L. García-Muñoz, J. Fontcuberta, C. Ritter, Phys. Rev. B 68, 012412 (2003)
[12] Q. Zhang, Z.F. Xu, H.B. Sun, X. Zhang, H. Wang, G.H. Rao, J. Alloys Compd. 745, 525 (2018)
[13] J.F. Wang, T.F. Shi, Z.T. Zhuang, Q.Q. Gao, Y.M. Zhang, RSC Adv. 8, 29071 (2018)
[14] Imad Hussain, M.S. Anwar, S.N. Khan, Jong Woo Kin, Kook Chae Chung, Bom Heun Koo, J. Alloys Compd. 694, 815 (2017)
[15] D. Serrate, J.M. De Teresa, J. Blasco, M.R. Ibarra, L. Morellón, C. Ritter, Appl. Phys. Lett. 80, 4573 (2002)
[16] D. Rubi, C. Frontera, J. Nogués, J. Fontcuberta, J. Phys.: Condens. Matter 16, 3173 (2004)
[17] C.L. Yuan, S.G. Wang, W.H. Song, T. Yu, J.M. Dai, S.L. Ye, Y.P. Sun, Appl. Phys. Lett. 75, 3853 (1999)
[18] S.R. Shinde, S.B. Ogale, R.L. Greene, T. Venkatesan, K. Tsoi, S.W. Cheong, A.J. Millis, J. Appl. Phys. 93, 1605 (2003)
[19] Y. Tomioka, T. Okuda, Y. Okimoto, R. Kumai, K. Kobayashi, Y. Tokura, Phys. Rev. B 61, 422 (2000)
[20] N. Kumar, G. Khurana, A. Gaur, R.K. Kotnala, J. Appl. Phys. 114, 053902 (2013)
[21] J. Zhang, W.J. Ji, J. Xu, Z.B. Gu, Y.B. Chen, S.T. Zhang, J. Phys.: Condens. Matter 31, 225001 (2019)
[22] D. Niebieskikwiat, A. Caneiro, R.D. Sánchez, J. Fontcuberta, Phys. Rev. B 64, 180406 (2001)
[23] D. Niebieskikwiat, A. Caneiro, R.D. Sánchez, J. Fontcuberta, Phys. B 320, 107 (2002)
[24] L. Harnagea, B. Jurca, P. Berthet, J. Solid State Chem. 211, 219 (2014)
[25] D.D. Sarma, S. Ray, K. Tanaka, M. Kobayashi, A. Fujimori, P. Sanyal, H.R. Krishnamurthy, C. Dasgupta, Phys. Rev. Lett. 98, 157205 (2007)
[26] E. Burzo, I. Balasz, S. Constantinescu, I.G. Deac, J. Magn. Magn. Mater. 316, e741 (2007)
[27] D. Niebieskikwiat, F. Prado, A. Caneiro, R.D. Sánchez, Phys. Rev. B 70, 132412 (2004)
[28] J.-F. Wang, B. Hu, J. Zhang, Z.-B. Gu, S.-T. Zhang, J. Alloys Compd. 621, 131 (2015)
[29] J.F. Wang, J. Zhang, B. Hu, Z.B. Gu, S.T. Zhang, J. Phys. D: Appl. Phys. 47, 445003 (2014)
[30] W. Zhong, W. Liu, C.T. Au, Y.W. Du, Nanotechnology 17, 250 (2006)
[31] M. Saloaro, S. Majumdar, H. Huhtinen, P. Paturi, J. Phys.: Condens. Matter 24, 366003 (2012)
[32] A. Nag, S. Jana, S. Middey, S. Ray, Indian J. Phys. 91, 883 (2017)
[33] F.J. Yue, S. Wang, L. Lin, H.F. Ding, D. Wu, Jo J. Phys. D: Appl. Phys. 45, 075001 (2012)
[34] S. Wang, F.J. Yue, D. Wu, F.M. Zhang, W. Zhong, Y.W. Du, Appl. Phys. Lett. 94, 012507 (2009)
[35] L. Xi, J.H. Du, J.H. Ma, Z. Wang, Y.L. Zuo, D.S. Xue, J. Alloys Compd. 550, 365 (2013)
[36] F.J. Yue, S. Wang, D. Wu, Appl. Phys. A 111, 347 (2013)

Figures

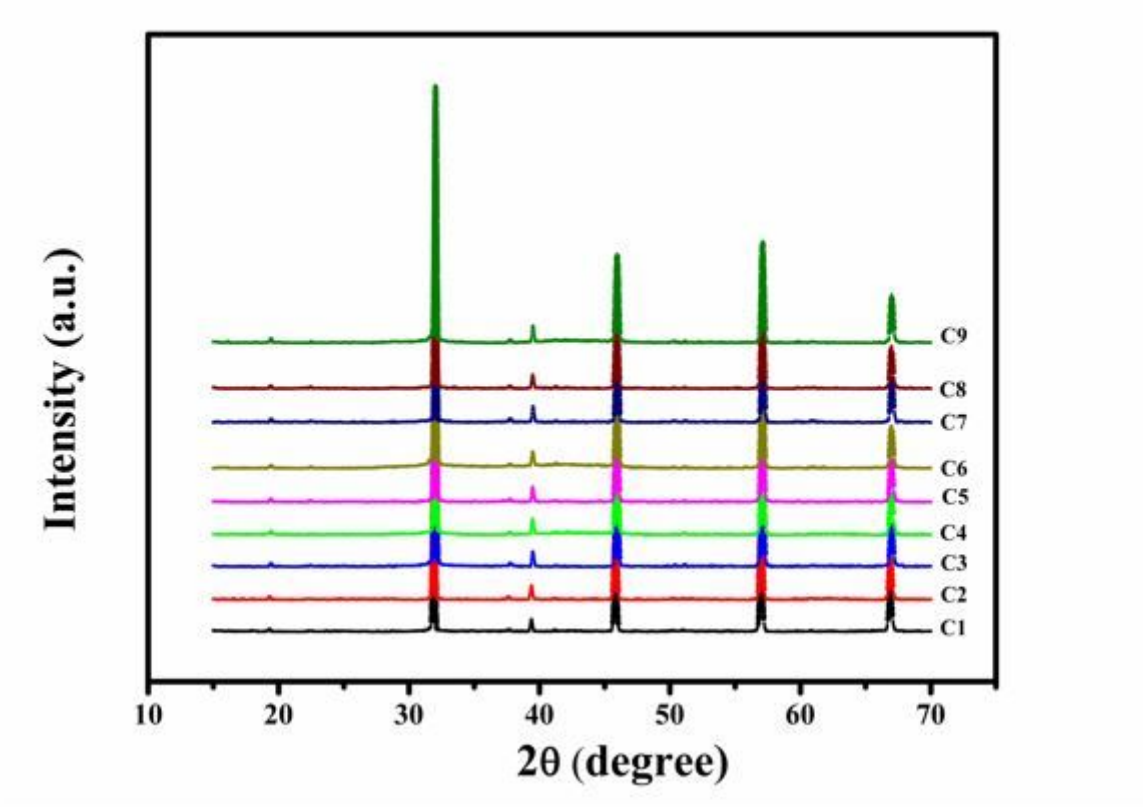

Figure 1

The XRD patterns of all prepared ceramics (C1-C9)

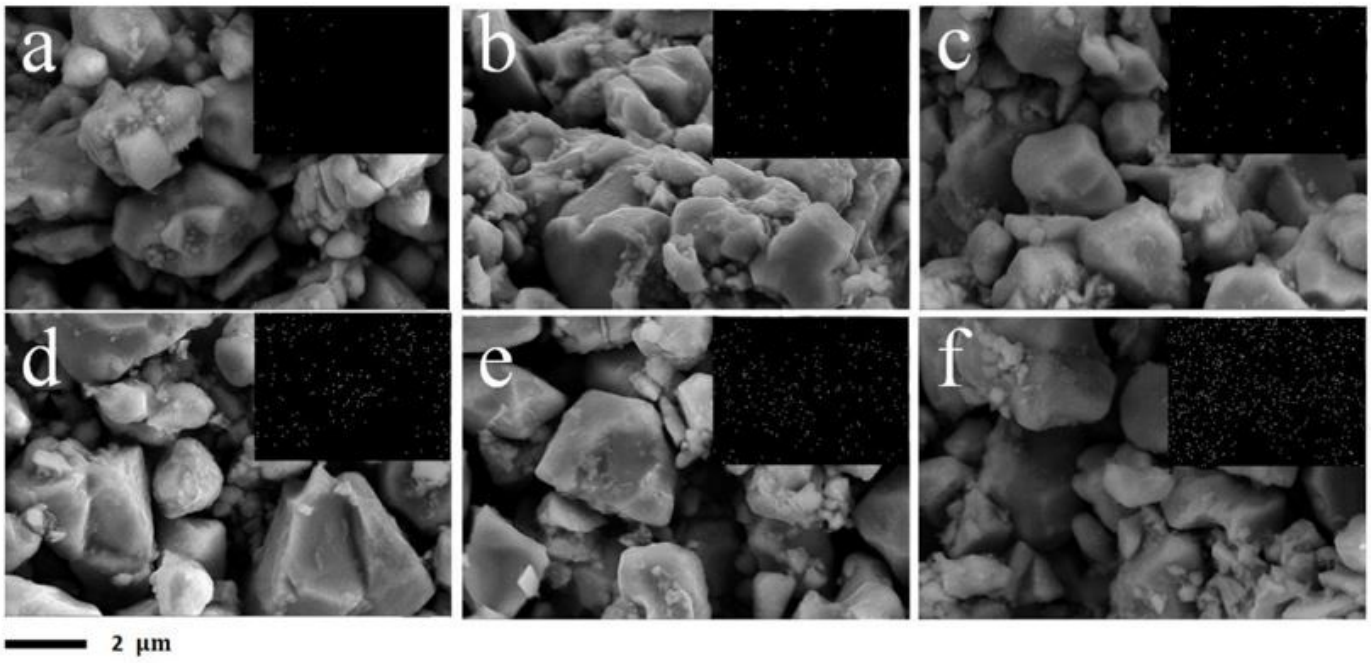

Figure 2

FESEM images of oleic acid/La0.5Sr1.5FeMoO6 composites, (a-f) correspond to C1-C6 samples. The insets are the corresponding C element mappings

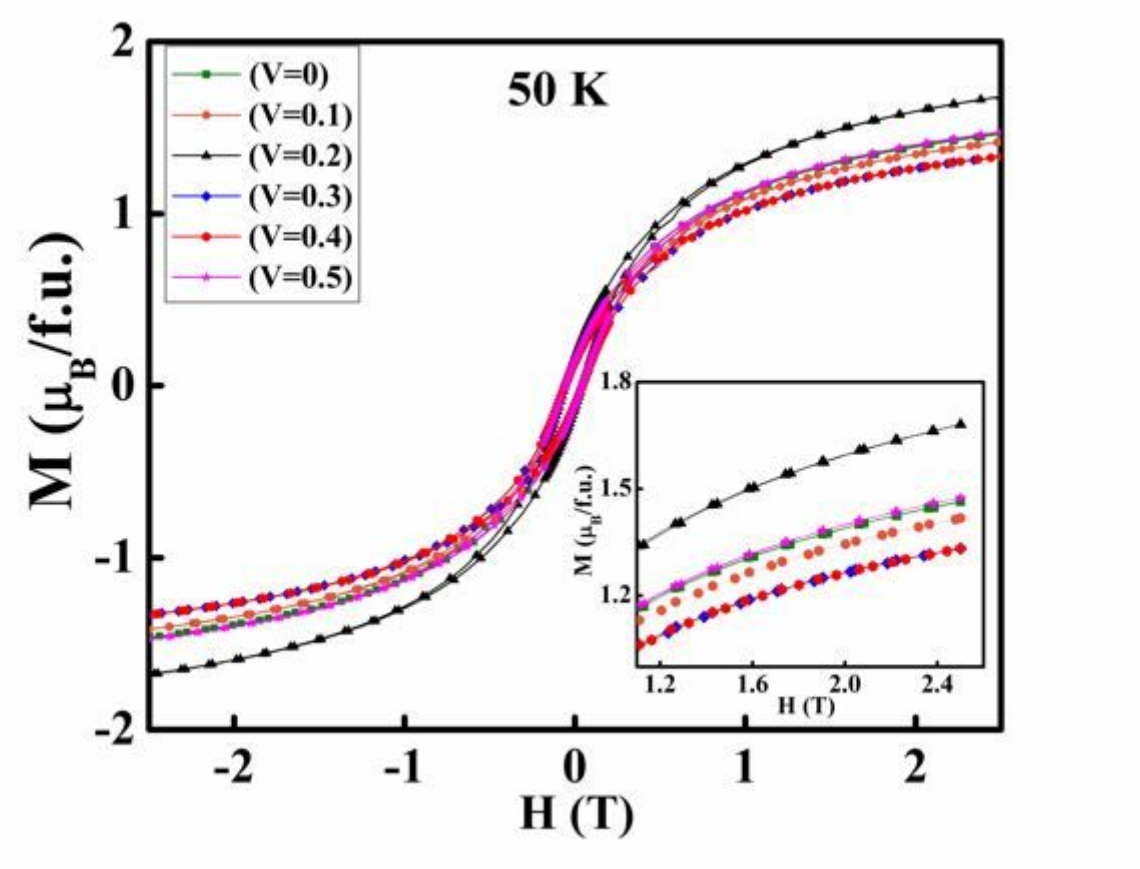

Figure 3

The magnetization versus magnetic field (M-H) curves measured at 50 K for Experiment Ⅱ. The inset is the locally enlarged M-H curves

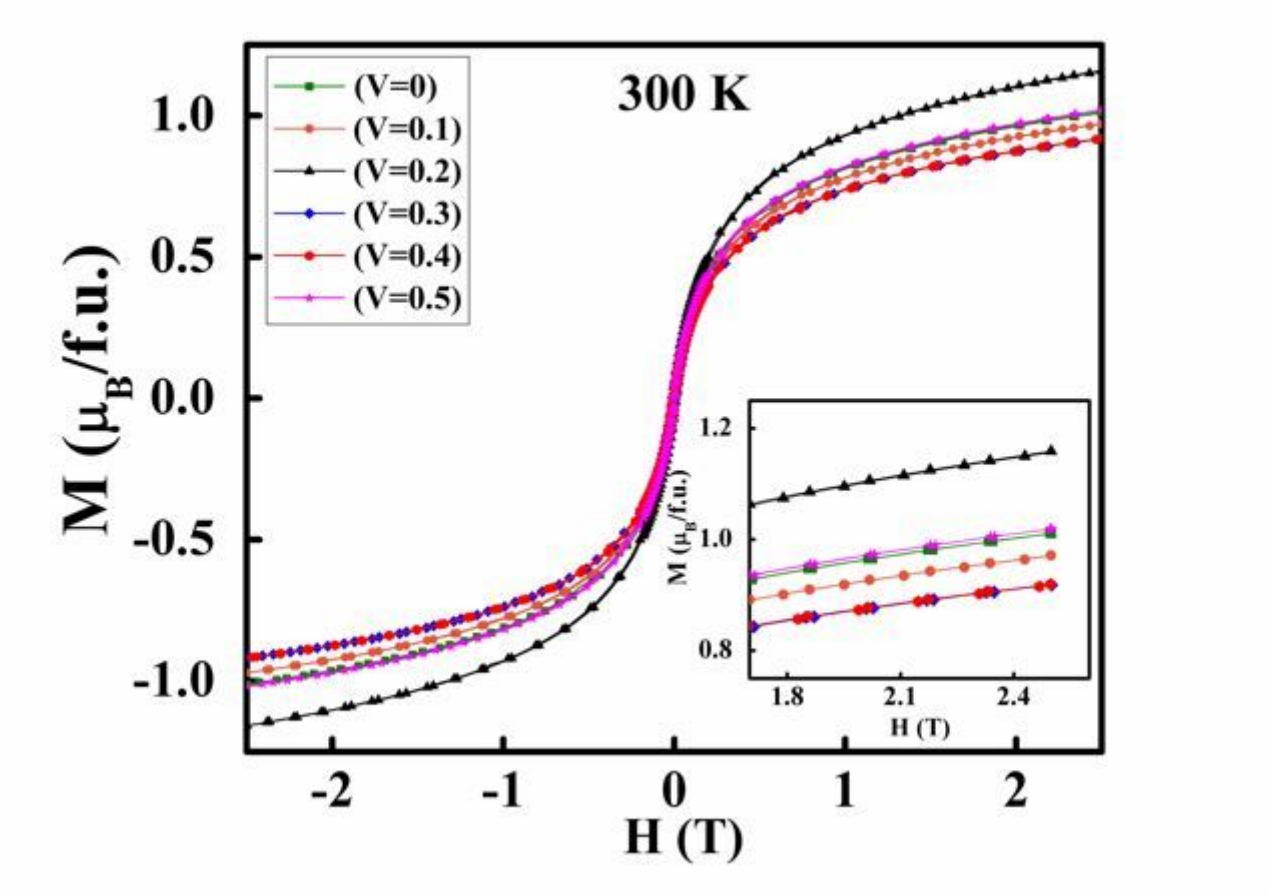

Figure 4

The magnetization versus magnetic field (M-H) curves measured at 300 K for C1-C6 in Experiment Ⅱ. The inset is the locally enlarged M-H curves

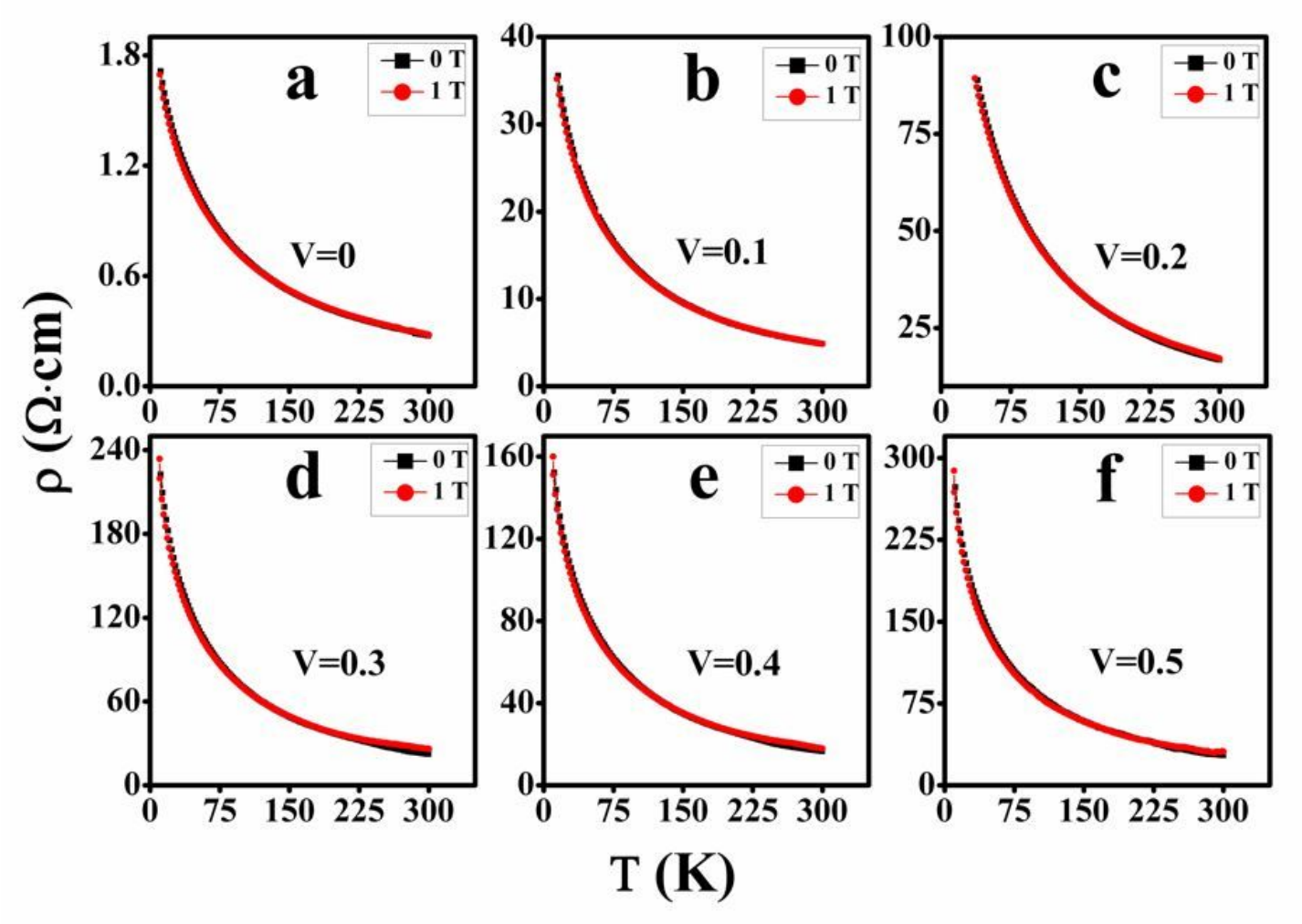

Figure 5

Temperature dependent resistivity curves for C1-C6 (a-f) measured at 10 K-300 K with 0 T and 1 T extra field

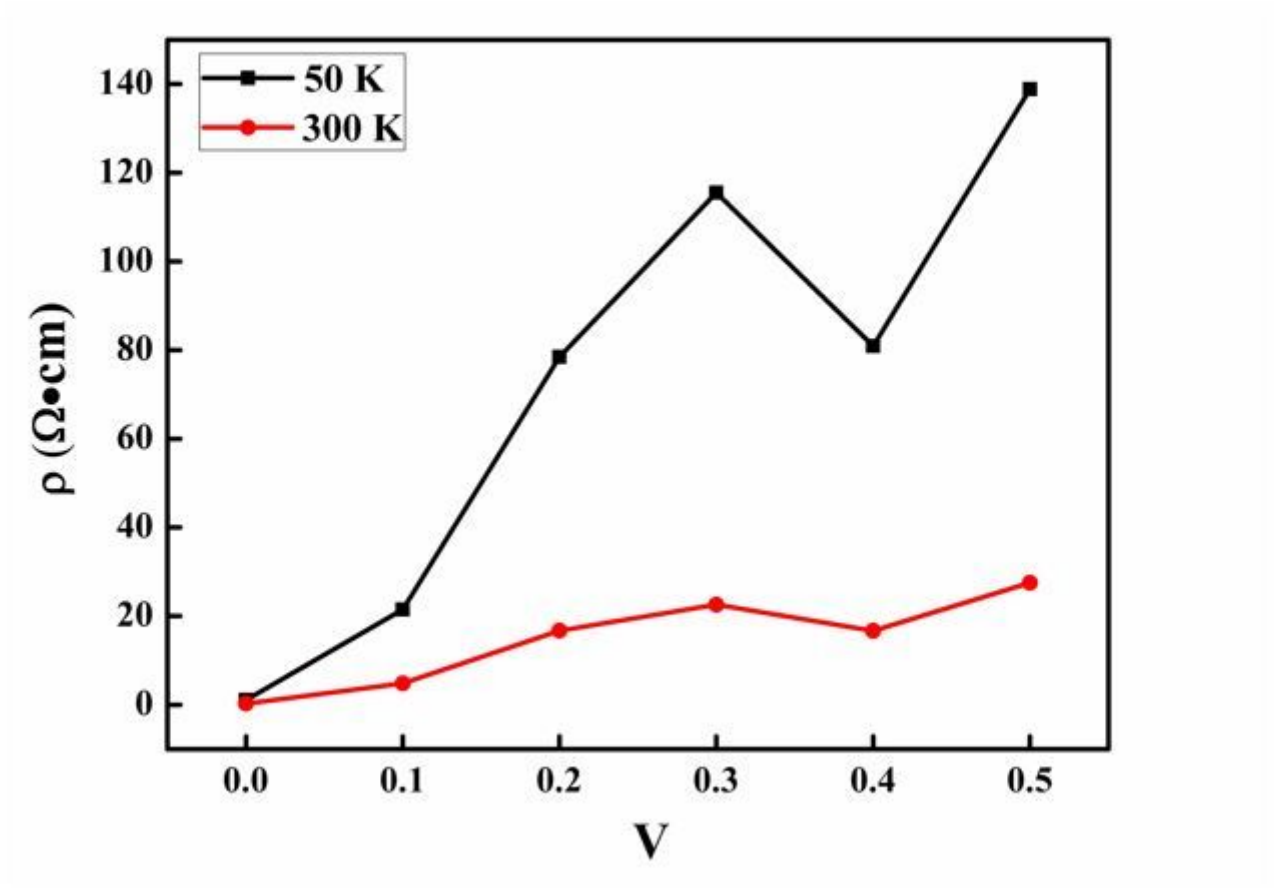

Figure 6

The resistivity-volume proportions curves of samples (C1-C6) at 50 K and 300 K with zero-field

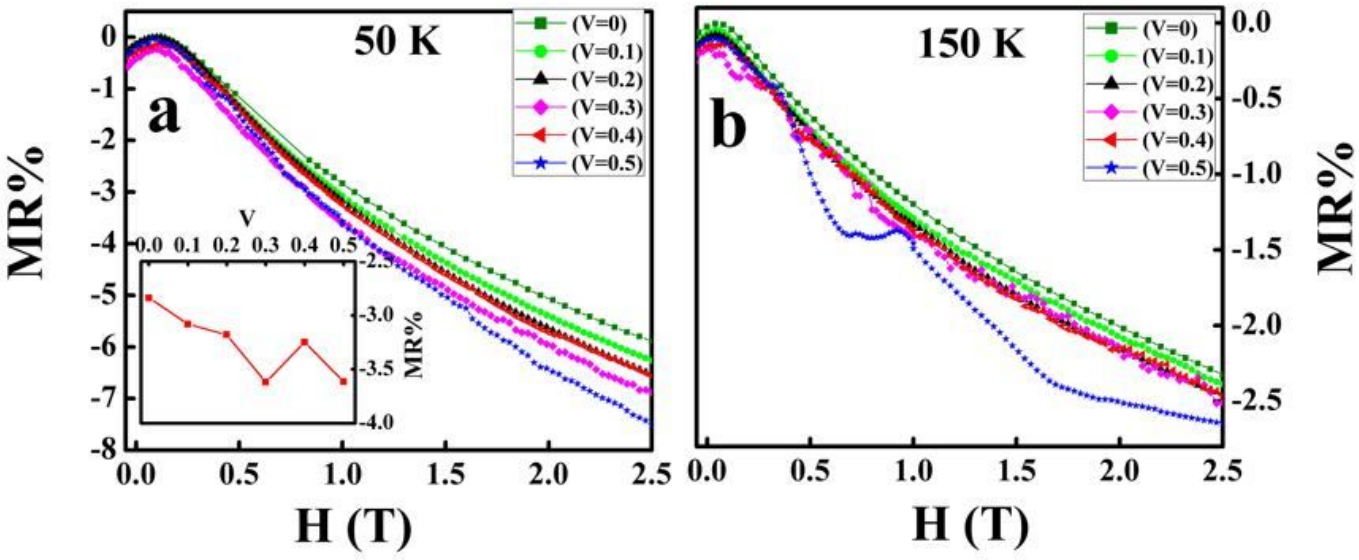

Figure 7

MR% versus applied magnetic field plots of La0.5Sr1.5FeMoO6 with different volume proportions of oleic acid/alcohol contents (V=0, 0.1, 0.2, 0.3, 0.4, 0.5) measured at 50 K (a) and 150 K (b). The inset in (a) was the volume proportions dependent MR at 1 T

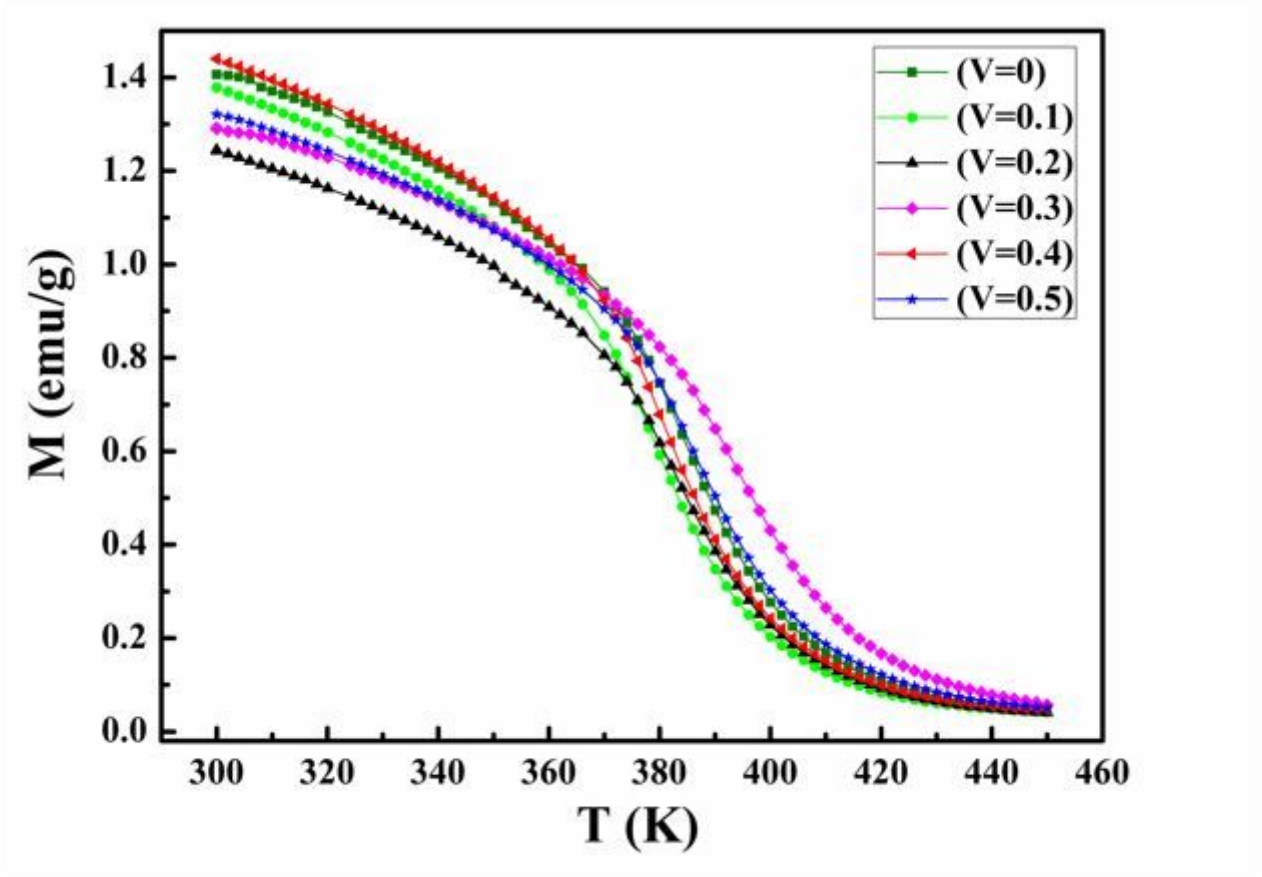

Figure 8

Magnetization-temperature (M-T) curves for C1-C6 measured from 300 K to 450 K

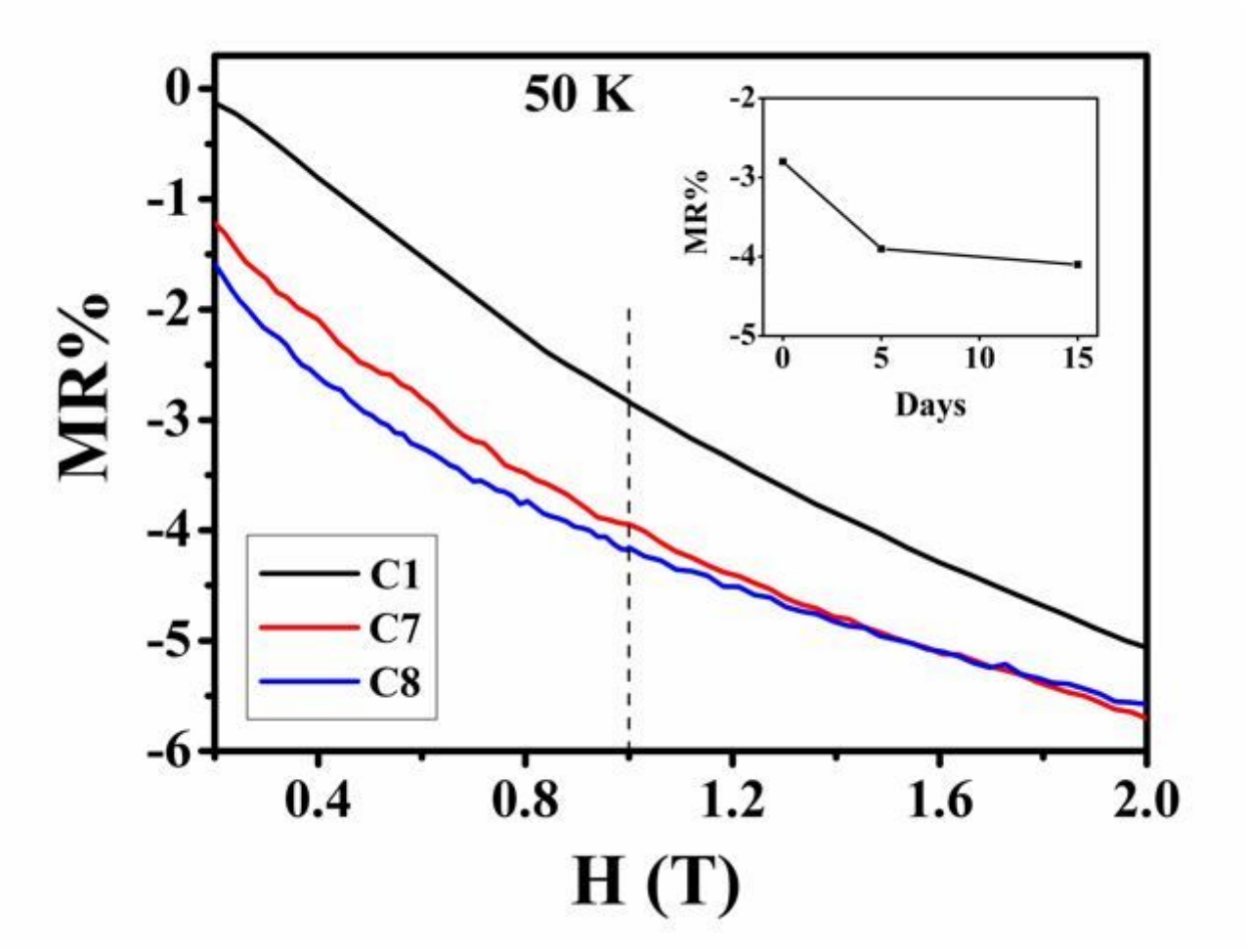

Figure 9

MR% versus applied magnetic field of C1, C7 and C8 measured at 50 K (Experiment). The inset is the LFMR value at 1 T of C1, C7 and C8

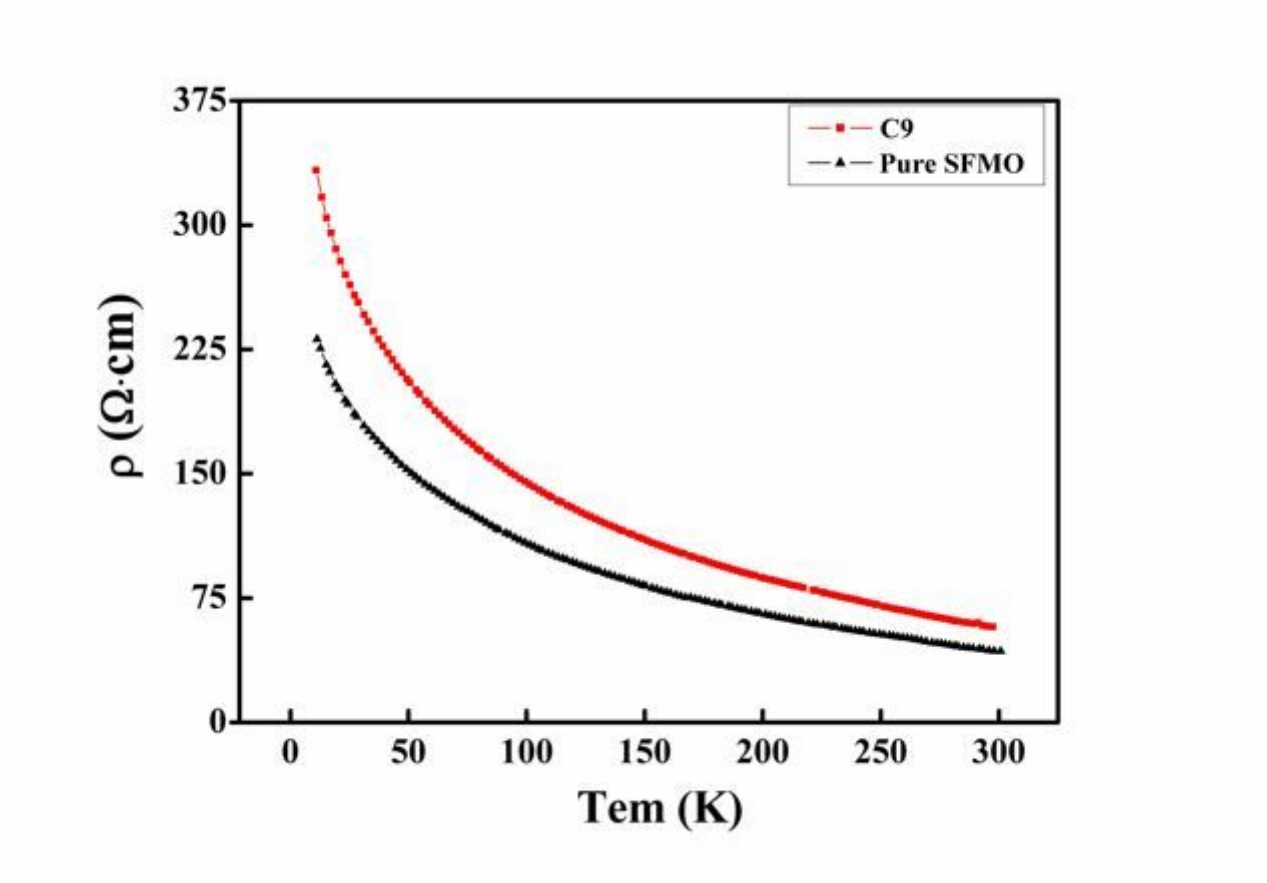

Figure 10

Resistivity versus temperature curves for pure SFMO and C9 at 10 K-300 K with zero-field

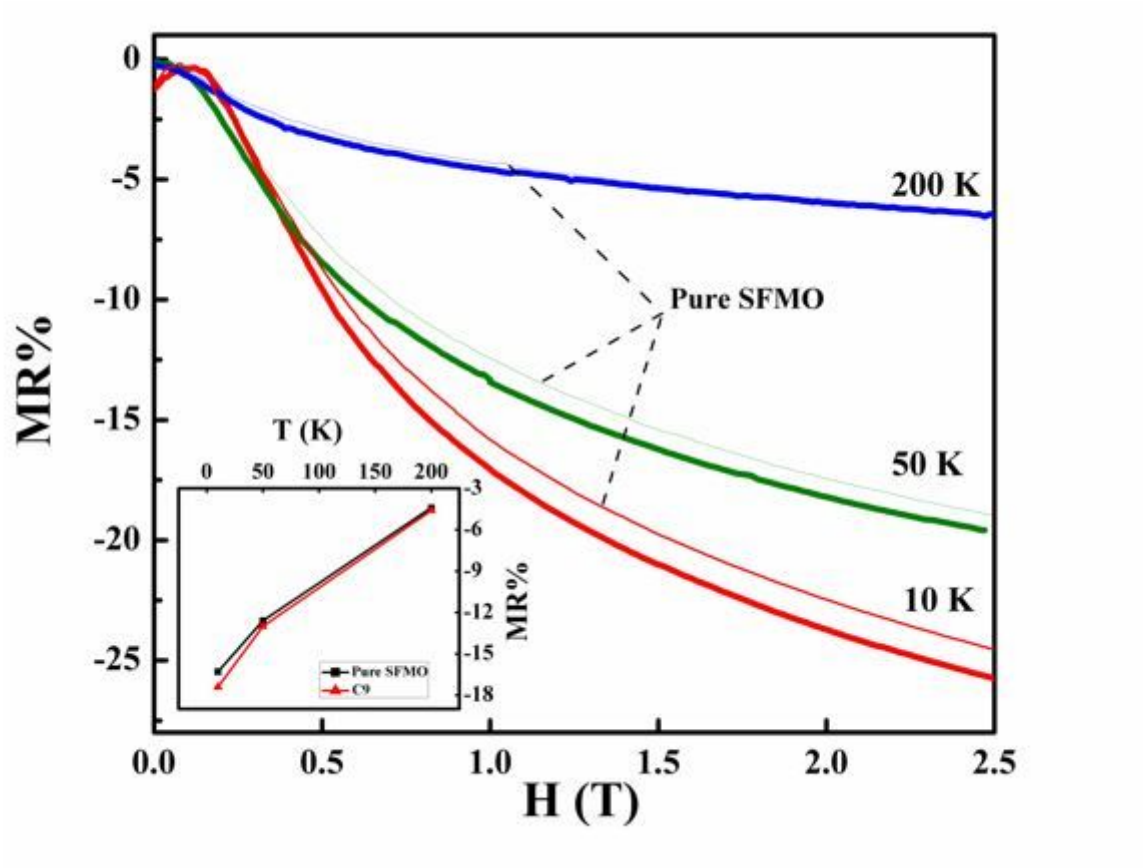

Figure 11

MR% versus applied magnetic field of pure SFMO sample (thin lines) and C9 (thick lines) measured at 10 K, 50 K and 200 K. The inset in figure is the measured temperature dependent low field magnetoresistance at 1 T for the two samples